

Fast Preemption: Forward-Backward Cascade Learning for Efficient and Transferable Preemptive Adversarial Defense

Hanrui Wang¹, Ching-Chun Chang¹, Chun-Shien Lu², Isao Echizen¹

¹National Institute of Informatics (NII); ²Academia Sinica

¹Tokyo, Japan; ²Taipei, Taiwan

¹{hanrui_wang, ccchang, iechizen}@nii.ac.jp; ²lcs@iis.sinica.edu.tw

Abstract

Deep learning has made significant strides but remains susceptible to adversarial attacks, undermining its reliability. Most existing research addresses these threats after attacks happen. A growing direction explores preemptive defenses like mitigating adversarial threats proactively, offering improved robustness but at cost of efficiency and transferability. This paper introduces Fast Preemption, a novel preemptive adversarial defense that overcomes efficiency challenges while achieving state-of-the-art robustness and transferability, requiring no prior knowledge of attacks and target models. We propose a forward-backward cascade learning algorithm, which generates protective perturbations by combining forward propagation for rapid convergence with iterative backward propagation to prevent overfitting. Executing in just three iterations, Fast Preemption outperforms existing training-time, test-time, and preemptive defenses. Additionally, we introduce an adaptive reversion attack to assess the reliability of preemptive defenses, demonstrating that our approach remains secure in realistic attack scenarios.

1. Introduction

Deep learning models are highly susceptible to adversarial attacks [18], enabling adversaries to manipulate media such as images, audio, and video. For instance, an attacker can alter a facial image’s identity without perceptible changes, bypassing facial authentication systems [44], or introduce imperceptible noise to traffic signs, potentially compromising autonomous driving safety [15]. Defending against such attacks remains a critical yet unresolved challenge.

Training-time and test-time defenses [6, 22, 26, 31] mitigate adversarial threats after attacks happen, improving robustness but reducing classification accuracy [51] and remaining vulnerable to adaptive attacks [7, 43]. In contrast, preemptive defenses [17, 29] preemptively modify media to

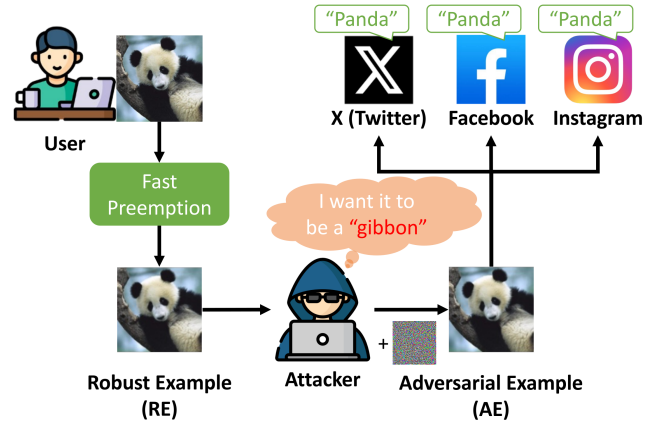


Figure 1. The proposed Fast Preemption offers transferable protection against an adversarial attack by preemptively manipulating the image before it is attacked.

neutralize future adversarial manipulations. However, preemptive defenses suffer from inefficiency and rely on paired protection-inference modules, limiting transferability. Additionally, the protection modules in preemptive defenses are dependent on the paired, provided models, rendering them susceptible to potential backdoor threats [36].

To address these challenges, we propose Fast Preemption, a novel preemptive defense illustrated in Fig. 1. Fast Preemption learns robust features, predicts potential adversarial perturbations, and amplifies these features while reversing the predicted perturbations, effectively neutralizing subsequent attacks. It offers six key advantages over other defenses:

- *No reliance on ground truths:* While ground-truth labels offer the highest protection, manual labeling is less practical. Fast Preemption operates without this requirement.
- *Plug-and-play:* Unlike training-time defenses, Fast Preemption requires no modifications to the classification system. Unlike existing preemptive defenses, it eliminates reliance on paired protection-inference modules, re-

ducing security and privacy risks associated with external model providers [16, 36].

- *Transferable*: Fast Preemption provides generalized protection without requiring prior knowledge of target models or attack algorithms.
- *Efficient*: A novel learning algorithm greatly improves efficiency compared to existing preemptive defenses.
- *State-of-the-art (SOTA) clean and robust accuracy*: Unlike training-time and test-time defenses, Fast Preemption enhances threat resistance without compromising classification accuracy. It achieves the best clean and robust accuracy among existing adversarial defenses.
- *Resilient to adaptive attacks*: Fast Preemption allows users to set protection strength and select a backbone model independently of the target model, enhancing resilience to adaptive attacks beyond existing test-time and preemptive defenses.

To achieve these objectives, we design Fast Preemption with three key components: a user-configurable classifier for automatic input labeling, a user-configurable backbone model (which may differ from the classifier) for feature learning, and a forward-backward (Fore-Back) cascade learning algorithm for efficiently computing transferable protective perturbations. The Fore-Back cascade learning algorithm integrates forward and backward propagation to overcome their individual limitations. Forward propagation ensures rapid convergence but overfits to the backbone model, reducing transferability. Conversely, backward propagation mitigates overfitting but requires many iterations, making it computationally expensive. By combining both, Fore-Back achieves efficient and robust protection.

We evaluate Fast Preemption on two datasets and thirteen models, defending against four representative adversarial attacks. Results demonstrate its superiority in clean and robust accuracy, transferability, and computational efficiency over benchmark training-time, test-time, and preemptive defenses. For example, on CIFAR-10 [23], Fast Preemption outperforms the SOTA preemptive defense [29], achieving 2.5% and 5.1% higher clean and robust accuracy, respectively, against AutoAttack (Standard) [11], while being 700 times faster.

We further explore stronger adaptive attack scenarios where the attacker has full knowledge of our defense and attempts to reverse its protective perturbations. Moon *et al.* [29] introduced the first reversion attack but failed, claiming their preemptive defense was irreversible. We propose *Preemptive Reversion*, a more powerful reversion attack that successfully bypasses their defense in a white-box setting (*i.e.*, both the defense algorithms and settings have been compromised). Preemptive Reversion applies a secondary preemptive defense to an already protected example and then reverses the newly introduced perturbations. Since the secondary defense generates perturbations similar to the

first under identical conditions, this process effectively evaluates a defense’s susceptibility to reversion.

We employ Preemptive Reversion alongside methods such as blind JPEG distortion and adversarial purification [31] to assess the reliability of Fast Preemption against adaptive attacks. Since Fast Preemption allows for user-configurable parameterization (*e.g.*, selection of the backbone model), and these configurations remain confidential, all adaptive attacks fail to bypass its protection, highlighting its robustness. However, in the less-realistic scenario where the user configurations are compromised, only Preemptive Reversion successfully removes the protective perturbations without introducing significant distortion, demonstrating the aggressiveness of the proposed attack. To our knowledge, Preemptive Reversion remains the only viable approach for evaluating the reliability of preemptive defenses against adaptive attacks.

We summarize our contributions as follows: (i) We introduce Fast Preemption, a more effective plug-and-play preemptive defense that requires neither ground truths nor prior knowledge of attacks or target models, while also providing resistance to adaptive attacks. (ii) We propose the Fore-Back cascade learning algorithm, which significantly enhances the transferability and learning speed of preemptive defenses. (iii) We develop Preemptive Reversion, a more robust tool for evaluating the reliability of preemptive defenses against adaptive attacks.

2. Related Works

Existing adversarial defenses can be classified into three main categories: training-time, test-time, and preemptive defenses.

Training-time defenses aim to develop robust deep learning models that can correctly classify adversarial examples (AEs) based on their ground truth labels [6, 13, 14, 18, 19, 26, 32, 38–40, 47, 51]. However, they have two key limitations. First, they require large amounts of high-quality, diverse data for training. Second, training-time defenses often sacrifice clean accuracy to improve robust accuracy.

Test-time defenses are divided into confusion, detection, and purification. Confusion methods integrate multiple layers or models, so that if an attacker bypasses one, other layers can resist the threat [3, 42]. However, Alfara *et al.* [42] and Wang *et al.* [44] acknowledge that this strategy is vulnerable when the attacker is aware of the defense and targets all layers in a single attack. Detection models identify AEs by distinguishing them from benign inputs [9, 22, 24, 53], but detection is challenging for unseen attacks, as detectors are often trained on known AEs. Furthermore, detection may misclassify benign images as AEs, reducing clean accuracy. In contrast, adversarial purification aims to remove perturbations in AEs. Early approaches used image distortion for purification [20, 34, 45], while recent methods gen-

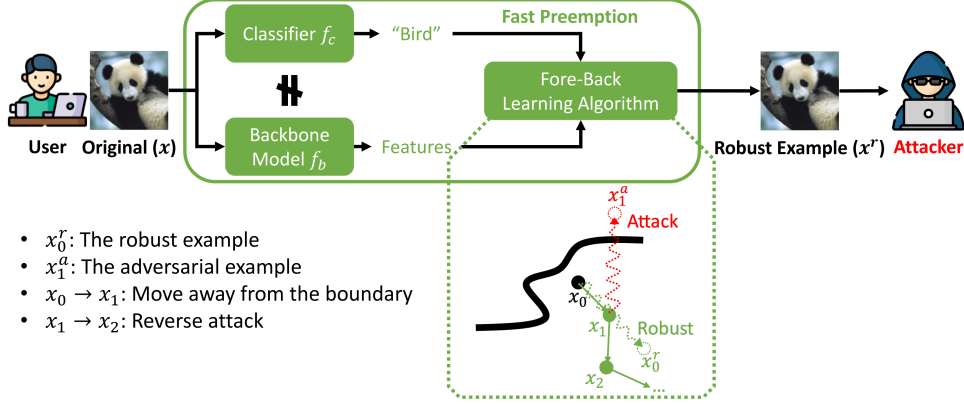


Figure 2. Fast Preemption framework. The classifier labels inputs automatically, which improves clean accuracy and thereby improves defense performance. The backbone model learns crucial features, so it must be adversarially trained. The Fore-Back learning algorithm first runs forward propagation ($x_0 \rightarrow x_1$) to quickly move away from the incorrect classes and then runs backward propagation ($x_1 \rightarrow x_2$) to alleviate overfitting on the backbone model.

erate benign replacements regardless of input type [31, 35]. A key limitation of purification is that the difference between original and generated examples can degrade clean accuracy, and counterattack potential remains [7, 43].

Preemptive defenses aim to generate robust examples (REs) that replace the original images, which are then discarded [17, 29, 37]. These REs are inherently more resilient to manipulation, offering resistance against adversarial attacks. However, these approaches face significant limitations, including high computational costs, limited transferability across models, and, in some cases, reduced robustness compared to other defense mechanisms.

3. Preemptive Defense: Fast Preemption

With the preemptive defense strategy, the image is preemptively “attacked” (manipulated for enhancement), protecting it before being attacked. In this section, we present the framework and algorithm of our Fast Preemption strategy.

3.1. Problem Definition

Adversarial attacks and preemptive defenses both manipulate inputs by adding subtle perturbations. Specifically, let x and y denote the original image and its ground-truth label, respectively, and let f_v denote the victim model. Let x' denote the manipulated example (AE or RE), formulated as

$$x' = x + \delta, \text{ s.t. } \|\delta\|_p \leq \epsilon, \quad (1)$$

where δ denotes the perturbations, $\|\cdot\|_p$ represents the L_2 - or L_∞ -norm and ϵ is the setting of the maximum distance. Therefore, adversarial attacks and preemptive defenses aim to solve different optimization problems (as explained below) by changing δ with the inputs of x , y , and f_v .

3.1.1. Adversarial Attack

An adversarial attack leads to misclassification due to subtle perturbations. Given an original image x and its ground truth y , the adversarial attacker is able to generate an AE by maximizing the cross entropy (CE) loss of x for label y , thereby reducing the model’s confidence in correctly classifying the input as its true label. Therefore, the optimization objective of an adversarial attack for misclassification is

$$\arg \max_{\delta} CE(f_v(x + \delta), y). \quad (2)$$

3.1.2. Preemptive Defense

A preemptive defense aims to generate REs those will make Eq. (2) less successful. With the preemptive defense strategy, “backward propagation optimization” is used to reverse the adversarial attack perturbations [29]. In other words, the optimization of Eq. (2) remains, but output δ is reversed. The backward propagation optimization is formulated as

$$\arg \max_{\delta} CE(f_v(x - \delta), y). \quad (3)$$

In contrast to backward propagation optimization, we newly define “forward propagation optimization” for the preemptive defense strategy. It directly reverses the optimization direction of Eq. (2) from maximization to minimization, which in turn enhances the model’s confidence in accurately classifying the input according to its true label:

$$\arg \min_{\delta} CE(f_v(x + \delta), y). \quad (4)$$

3.2. Framework

As illustrated in Fig. 2, the Fast Preemption framework includes three components.

Classifier: Correct input labels determines the correct optimization direction for defense. However, for efficient user interaction, it is less practical to label each input manually. Classifier f_c labels these inputs automatically. Therefore, y in Eq. (3) and Eq. (4) can be replaced by $f_c(x)$. The framework is integrated with user application before being attacked, so f_c does not have to show any transferability or resistance against threats, but it must offer the best classification accuracy. Processing images with ground truths can be regarded as using a perfect classifier.

Backbone Model: With Fast Preemption, the input image is iteratively optimized on backbone model f_b , which may differ from victim model f_v in Eq. (3) and Eq. (4). Therefore, due to its complexity, f_b determines the transferable clean and robust accuracies and time cost. To achieve better performance, the backbone model f_b must be adversarially trained so it can learn more crucial features instead of random pixels. The limitations of adversarially trained models (*i.e.*, training-time defenses), such as the degradation of clean accuracy, are alleviated by the well-performing nonrobust classifier f_c in our framework. As a result, the preemptive defense optimizes the inputs towards the correct labels. Therefore, two different models, classifier f_c and backbone f_b , are integrated into the framework.

Fore-Back Cascade Learning Algorithm: To meet our framework, the optimization problems formulated as Eq. (3) and Eq. (4) can be reformulated as

$$\arg \max_{\delta} CE(f_b(x - \delta), f_c(x)), \quad (5)$$

$$\arg \min_{\delta} CE(f_b(x + \delta), f_c(x)), \quad (6)$$

respectively, where f_c is our classifier and f_b is our backbone model. This cascade learning algorithm is described in detail in the next section.

3.3. Forward-Backward Cascade Learning

The Fore-Back cascade learning algorithm is used to compute protective perturbations. The input is first moved away from the classification boundaries of all incorrect classes so that the manipulated input will be easier to be classified as the ground truth. We define this as *forward propagation* (\rightarrow). Forward propagation can quickly attain convergence (less time cost) but causes overfitting on the backbone model so that the defense is less transferable to other victim models. *Backward propagation* optimization (\leftarrow) is thus conducted following forward propagation. Backward propagation reverses the adversarial perturbations to make them protective perturbations, which effectively alleviates overfitting and thereby improves transferability. In summary, the forward and backward propagation both enhance robustness, but in different optimization directions. The complete algorithm is presented in Algorithm 1 of Appendix A.

3.3.1. Loss Function

From Eq. (5) and Eq. (6), the loss function of our Fore-Back cascade learning algorithm is the CE loss:

$$\ell(x_i|x, f_c, f_b) = CE(f_b(x_i), f_c(x)), \quad (7)$$

where x_i and x denote the output example of the i -th iteration and the original input, respectively, and f_c and f_b are our classifier and backbone models, respectively. The forward optimization reduces ℓ , while the backward optimization increases it.

3.3.2. Preliminary - Backward Propagation

The use of backward propagation for preemptive defense was introduced in the SOTA preemptive defense strategy [29]. At each step of that strategy, a projected gradient descent (PGD) attack [28] is run first as $x_1 \rightarrow x_1^a$ (Fig. 2), and then the adversarial perturbations are reversed in accordance with the learning rate and thereby forms protective perturbations, as $x_1 \rightarrow x_2$.

Specifically, backward propagation first runs an I -iteration L_∞ -norm PGD attack from x_t , which is the output of the previous optimization step (forward or backward). In other words, the backward propagation increases ℓ via

$$\begin{aligned} x_{t,0} &= x_t, \\ x_{t,i+1} &= \prod_{x,\epsilon} (x_{t,i} + \alpha \cdot \text{sign}(\nabla \ell(x_{t,i}|x, f_c, f_b))), \quad (8) \\ \text{s.t. } & \|x_{t,i+1} - x\|_\infty \leq \epsilon \ \& \ 0 \leq i < I - 1, \end{aligned}$$

where ϵ is the setting of the maximum distance and α is the step size. The final output of Eq. (8) is AE x_t^a . Next, backward propagation subtracts perturbations $x_t^a - x_t$ from x_t in accordance with learning rate η , thereby computing the next RE, x_{t+1} :

$$\begin{aligned} x_{t+1} &= \prod_{x,\epsilon} (x_t - \eta \cdot (x_t^a - x_t)) \\ &= \prod_{x,\epsilon} (x_t - \eta \cdot \alpha \cdot \sum_{i=1}^I \text{sign}(\nabla \ell(x_{t,i}|x, f_c, f_b))). \quad (9) \end{aligned}$$

The SOTA preemptive defense strategy [29] relies solely on backward propagation learning, which requires multiple steps to converge due to the random initialization of adversarial attacks (at least ten steps). In contrast, the Fast Preemption strategy accelerates defense by incorporating forward propagation before backward propagation learning.

3.3.3. Combining Forward and Backward Propagation

We define forward propagation learning as a direct enhancement by moving away from the decision boundary in accordance with the learning rate ($x_0 \rightarrow x_1$ in Fig. 2). Therefore,

it first reduces ℓ via

$$\begin{aligned} x_{t,0} &= x_t, \\ x_{t,i+1} &= \prod_{x,\epsilon} (x_{t,i} - \alpha \cdot \text{sign}(\nabla \ell(x_{t,i}|x, f_c, f_b))), \quad (10) \\ \text{s.t. } & \|x_{t,i+1} - x\|_\infty \leq \epsilon \ \& \ 0 \leq i < I - 1, \end{aligned}$$

the final output of which is RE x_t^r . Subsequently, protective perturbations $x_t^r - x_t$ are directly added to x_t in accordance with learning rate η :

$$\begin{aligned} x_{t+1} &= \prod_{x,\epsilon} (x_t + \eta \cdot (x_t^r - x_t)) \\ &= \prod_{x,\epsilon} (x_t - \eta \cdot \alpha \cdot \sum_{i=1}^I \text{sign}(\nabla \ell(x_{t,i}|x, f_c, f_b))), \quad (11) \end{aligned}$$

which is the same as for Eq. (9). Therefore, the above derivations can be summarized as

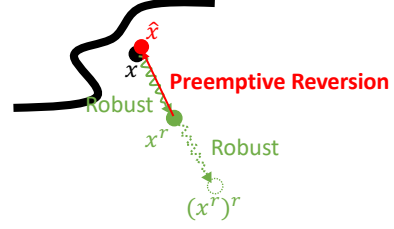
$$\begin{aligned} x_{t,0} &= x_t, \\ x_{t,i+1} &= \begin{cases} \prod_{x,\epsilon} (x_{t,i} - \alpha \cdot \text{sign}(\nabla \ell(x_{t,i}|x, f_c, f_b))) & \rightarrow \\ \prod_{x,\epsilon} (x_{t,i} + \alpha \cdot \text{sign}(\nabla \ell(x_{t,i}|x, f_c, f_b))) & \leftarrow \end{cases} \\ x_{t+1} &= \prod_{x,\epsilon} (x_t - \eta \cdot \alpha \cdot \sum_{i=1}^I \text{sign}(\nabla \ell(x_{t,i}|x, f_c, f_b))), \\ \text{s.t. } & \|x_* - x\|_\infty \leq \epsilon \ \& \ 0 \leq i < I - 1, \quad (12) \end{aligned}$$

where x_* denotes $x_{t,i+1}$ or x_{t+1} . Eq. (12) indicates that both forward and backward propagation make inputs more robust but with different learning directions for loss ℓ .

Whereas backward propagation requires many steps to converge, forward propagation converges quickly. However, forward propagation causes overfitting of the backbone model, so the defense will be less transferable to other victim models. Fast Preemption alleviates this overfitting: T_{\rightarrow} steps of forward propagation are run until there is slight overfitting; then T_{\leftarrow} steps of backward propagation are run to eliminate the overfitting. We evaluated whether the learning is overfitted by evaluating transferability. With this combination of forward and backward propagation, Fast Preemption attains SOTA performance with only three steps (one step T_{\rightarrow} , followed by two steps T_{\leftarrow}), which dramatically reduces the time cost of RE generation.

3.3.4. Averaging N Examples

Forward and backward propagation both require a backbone optimization algorithm, *i.e.*, an adversarial attack algorithm. For example, The Bi-Level optimization [29] used PGD [28] for backward propagation. However, PGD has to run many sequential iterations to compute superior adversarial perturbations, which greatly increases the time cost. With the Fast Preemption strategy, Fast Gradient Sign Method



- $x \rightarrow x^r$: Preemptive defense
- $x^r \rightarrow (x^r)^r$: Preemptive defense in same setting
- $\tilde{x} = x^r - ((x^r)^r - x^r)$: Assume preemptive defenses manipulating similar pixels

Figure 3. Illustration of Preemptive Reversion algorithm. It first conducts a secondary preemptive defense on RE x^r and then reverses the perturbations of the secondary defense: $(x^r)^r - x^r$.

(FGSM) [18] is used to speed up the computation of adversarial perturbations.

Since FGSM has difficulty obtaining optimal perturbations, with the Fast Preemption strategy, it is run N times with random initialization to produce N FGSM examples. The perturbations are then averaged to obtain the final output. We demonstrate that averaging the perturbations for PGD examples negligibly affects performance, whereas with the Fast Preemption strategy, FGSM optimization is effectively improved while efficiency is preserved.

Furthermore, averaging perturbations in the N FGSM examples is faster than processing a single example with iterative PGD. To generate a single RE, iterative PGD has to run each iteration sequentially from a single input, whereas N FGSM examples can be produced by repeating the single input N times and processing the results in parallel.

4. Adaptive Attack: Preemptive Reversion

A reversion attack is used to assess the reliability of a preemptive defense. While Moon *et al.* [29] first proposed a reversion attack against their proposed defense, Bi-Level, but failed to reverse it, claiming it was irreversible, we propose a stronger reversion attack successfully overcame Bi-Level. In this section, we present the algorithm for our proposed Preemptive Reversion and a more comprehensive protocol for evaluating the effectiveness of reversion attacks.

4.1. Algorithm

When running preemptive defenses sequentially for the same input and settings, the perturbations are mostly the same for two rounds (see Fig. 5). On the basis of this finding, we devised the adaptive reversion attack, *i.e.*, *Preemptive Reversion*, as illustrated in Fig. 3. The complete algorithm is presented in Algorithm 2 of Appendix A. Using RE x^r generated by a preemptive defense method, the Preemptive Reversion algorithm first runs a secondary preemptive

defense upon x^r to obtain $(x^r)^r$. Then, the Preemptive Reversion algorithm reverses the secondary perturbations from x^r to obtain \tilde{x} , which is the prediction of the original input x :

$$\tilde{x} = x^r - ((x^r)^r - x^r). \quad (13)$$

4.2. Attack Scenarios

We define two reversion attack scenarios via the attacker’s knowledge of the backbone model and defense algorithm:

- *White-Box*: The attacker has complete knowledge of both the backbone model and defense algorithm (including settings), enabling them to replicate the secondary defense. This scenario, while the strongest, is less realistic due to varying user settings.
- *Black-Box*: The attacker knows the defense algorithm (typically public) but lacks knowledge of the backbone model, which can vary across users. The challenge in this scenario is that the features learned in the secondary defense may differ from those learned by the user.

Our proposed Preemptive Reversion attack is effective for evaluating the reversibility of preemptive defenses, including Fast Preemption, but it is only feasible in the white-box scenario. Without full knowledge of the defense, Fast Preemption remains reliable.

4.3. Evaluation Protocol

If a reversion attack succeeds, clean accuracy should decrease. However, image distortion can lead to a similar outcome, meaning a drop in clean accuracy does not necessarily indicate a successful reversion. To address this, we propose a comprehensive protocol to distinguish successful reversion from distortion. First, we intentionally assign incorrect labels to partial inputs, ensuring the clean accuracy after defense is lower than the original. If clean accuracy approaches the original value, the reversion attack is successful; otherwise, the drop in accuracy is due to distortion.

5. Experiment Settings

Datasets, Classifier, and Backbone Models. We conducted experiments on two datasets: CIFAR-10 [23] and ImageNet [2]. For CIFAR-10, ResNeXt29-32x4d [21] and PreActResNet-18 [19] were selected as the classifier and backbone model, respectively. For ImageNet, DeiT Base [41] and ConvNeXt-L+ConvStem [40] were selected as the classifier and backbone model, respectively. The model architectures are listed in Tab. 5 of Appendix B.

Adversarial attacks. We evaluated defenses against four adversarial attacks: white-box attacks include AutoAttack [11] and Carlini-Wagner (CW) [7]; black-box attacks include Deformation-Constrained Warping (DeCoW) [25] and Meta Conditional Generator (MCG) [50]. For AutoAttack, we used both its “Standard” version (combining APGD-CE, APGD-DLR, FAB [10], and Square At-

tack [4]) and its “Random” version (combining APGD-CE and APGD-DLR, with expectation over time (EOT) equal to 20 [5]). **Reversion attacks.** We examined: (i) whether protected samples induced by preemptive defenses cannot be easily reversed to their original unprotected state, which we define as “irreversible”; and (ii) the effectiveness of the proposed adaptive reversion attack, Preemptive Reversion. Along with Preemptive Reversion, we also ran reversion attacks using blind distortion (JPEG compression) and adversarial purification (DiffPure [31]).

Training-time defenses. We compared Fast Preemption with WideResNet-94-16 [6] and Swin-L [26] on the CIFAR-10 and ImageNet datasets, respectively. The architectures of these models differ from the backbone models. To assess the transferability of preemptive defenses, we conducted experiments across additional nine victim models, with results presented in Tab. 6 of Appendix C. **Test-time defenses.** We used DiffPure [31] as the benchmark test-time defense. The inputs were purified by DiffPure and then fed into WideResNet-94-16 [6] or Swin-L [26] depending on the dataset. **Preemptive defenses.** We compared Fast Preemption with the SOTA preemptive defense, Bi-Level [29], and the latest preemptive defense, A^5 [17].

Evaluation metrics. We evaluated performance using clean accuracy and robust accuracy, where higher values indicate better defense effectiveness. Clean accuracy was computed for benign images (original and REs), while robust accuracy was computed for AEs. Additionally, to assess image quality, we calculated the structural similarity index measure (SSIM) [46] and Learned Perceptual Image Patch Similarity (LPIPS) [52] relative to the original images. Higher SSIM and lower LPIPS values indicate subtler changes in the images.

6. Performance

The experiments were conducted using the settings outlined in Tab. 4 of Appendix B. Time costs were recorded on an NVIDIA A100 40GB GPU.

6.1. Robustness against Adversarial Attacks

We evaluated transferable defense performance under the condition, where the defense lacks knowledge of both the attacks and victim models [6, 26]. Tab. 1 and Tab. 2 compares Fast Preemption with benchmark defenses against four attacks. Fast Preemption outperformed the benchmarks in both clean and robust accuracies while maintaining competitive time costs. For instance, compared to the least time-costly method, WideResNet-94-16 [6] on CIFAR-10 under Standard L_∞ AutoAttack, Fast Preemption achieved 1.6% and 11.9% higher clean and robust accuracies, respectively, with only a marginal increase of 0.04 seconds per generation. Compared to the SOTA preemptive defense Bi-Level [29], which had the second-best accuracy, Fast Pre-

Table 1. End-to-end performance against AutoAttack [11] and comparison with benchmark adversarial defenses.

Dataset	Defense	Time Cost (s)	Clean (%)	Standard L_∞ (%)	Standard L_2 (%)	Random L_∞ (%)	
CIFAR-10	Training-Time	WideResNet-94-16 [6]	0	93.4	74.6	69.6	74.8
	Test-Time	DiffPure [31]	0.3	91.4	78.1	84.9	78.4
	Preemptive	A^5 [17]	0.01	93.5	73.8	69.0	74.3
		Bi-Level [29]	28	92.5	81.4	78.6	81.6
		Fast Preemption (ours)	0.04	95.0	86.5	84.3	86.7
	Combination	Ours+[31]	0.34	94.2	89.1	92.8	89.7
ImageNet	Training-Time	Swin-L [26]	0	93.0	67.0	59.5	67.5
	Test-Time	DiffPure [31]	1.2	88.8	73.7	79.4	73.8
	Preemptive	Bi-Level [29]	43	93.6	71.5	62.8	72.3
		Fast Preemption (ours)	1.3	95.1	77.1	67.4	78
		Combination	Ours+[31]	2.5	93.3	82.9	87.6

Bold indicates the best performance.

Table 2. Robust accuracy (%) against various adversarial attacks with L_∞ -norm perturbations and $\epsilon = 8/255$.

Threat Model	Attack	WideResNet-94-16	Bi-Level	Ours
White-Box	AutoAttack	74.0	82.1	86.5
	CW	80.8	85.4	90.3
Black-Box	DeCoW	88.8	89.7	93.6
	MCG	76.1	83.3	87.3

AutoAttack is the standard version. **Bold** indicates the best performance.

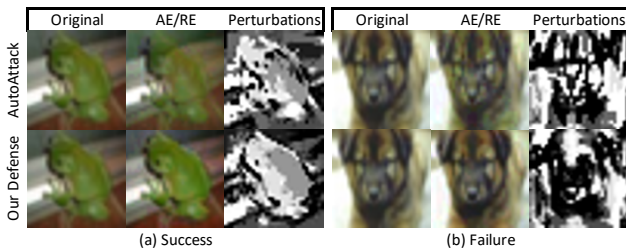


Figure 4. Perturbations of adversarial attacks and preemptive defenses. Visual comparison between the original image and the robust example (RE) shows that Fast Preemption perturbations are imperceptible. Furthermore, comparison of perturbations between AutoAttack and Fast Preemption indicates that the preemptive defense is more likely to succeed when perturbations are similar.

emption improved clean and robust accuracies by 2.5% and 5.1%, respectively, while being 700 times faster. Notably, preemptive defenses can be combined with training- and test-time defenses. For example, when paired with a test-time defense, Fast Preemption’s performance was significantly enhanced, as shown in the final rows of CIFAR-10 and ImageNet in Tab. 1.

Fig. 4 provides a qualitative analysis, comparing the original images with their corresponding REs. The perturbations introduced by Fast Preemption are barely perceptible. The average SSIM and LPIPS scores for 2,000 examples from CIFAR-10 and ImageNet are 0.97 and 0.01,

respectively, both surpassing those of AutoAttack and the SOTA preemptive defense Bi-Level [29] (more details in Appendix D). Additionally, the “Success” and “Failure” cases indicate that preemptive defense is more likely to succeed when the perturbations closely resemble those of the attack. The perturbation illustration δ_{Gray} was generated by normalizing the true perturbations δ from $[-\epsilon, +\epsilon]$ to $[0, 1]$, converting δ_{RGB} to grayscale using the NTSC formula [27].

$$\begin{aligned} \delta_{RGB} &= \frac{\delta + \epsilon}{2 \cdot \epsilon}, \\ \delta_{Gray} &= 0.299 \cdot \delta_{RGB.R} + \\ &\quad 0.587 \cdot \delta_{RGB.G} + 0.114 \cdot \delta_{RGB.B}, \end{aligned} \quad (14)$$

where $\delta_{RGB.R}$, $\delta_{RGB.G}$, and $\delta_{RGB.B}$ represent the red, green, and blue channels, respectively.

6.2. Resistance against Reversion Attacks

We conducted reversion attacks to assess the reversibility of preemptive defenses. In addition to the proposed Preemptive Reversion attack, we employed JPEG compression and adversarial purification, which do not require knowledge of the defense. Preemptive Reversion was tested in both white-box and black-box scenarios (see Sec. 4.2). The results, summarized in Tab. 3, reveal that only Preemptive Reversion, indicated in red, succeeded in reversing the preemptive defense, bringing the accuracy closer to the original. Other reversion attacks failed, further degrading clean accuracy due to distortion.

Notably, Preemptive Reversion is effective only in the white-box setting, which is less realistic for our preemptive defense, as our defense allows confidential user configurations (e.g., selection of the backbone model). In the black-box setting, where the backbone models are unknown, all adaptive attacks fail to bypass the preemptive defense, further demonstrating its reliability. In contrast, other preemptive defenses, such as Bi-Level [29], rely on paired protection-inference models, meaning that compromising the target model is sufficient to reverse user protections.

Table 3. Preemptive defenses resist reversion attacks.

Original (%)	Classifier	Preemptive Defense		Clean (%)	Distortion JPEG (%)	Purification DiffPure (%)	Preemptive Reversion (ours)	
		Backbone	Approach				White (%)	Black (%)
93.5	Bi-Level	Bi-Level	Bi-Level	91.9	90.5	90.8	93.1	90.7
	Bi-Level	PreActResNet-18	Bi-Level	91.2	90.6	90.7	93.4	91.0
	Bi-Level	PreActResNet-18	Ours	91.3	90.5	90.5	93.4	90.6
	ResNeXt29-32x4d	PreActResNet-18	Ours	95.5	94.4	94.8	94.0	94.6

Numbers in red demonstrate that only our reversion attack is feasible but only in the white-box setting.

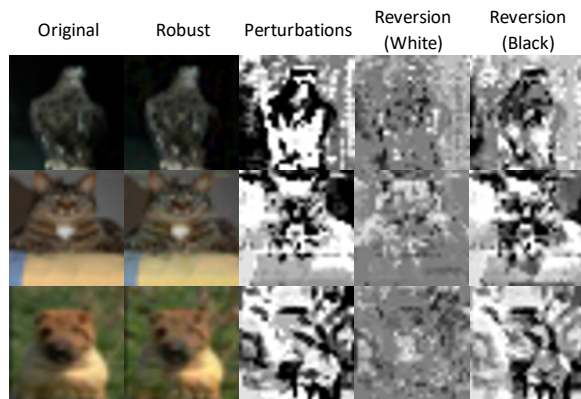


Figure 5. Perturbations before and after proposed Preemptive Reversion attack. White-box reversion successfully erased most protective perturbations while black-box reversion failed.

Fig. 5 corroborates our findings, showing that the white-box reversion successfully eliminates most protective perturbations, whereas the black-box reversion fails. However, due to the randomization inherent in Fast Preemption (*i.e.*, randomly initialized FGSM), the white-box reversion cannot entirely remove all protective perturbations. The fourth row in Tab. 3, which was obtained without our evaluation protocol, further highlights the comprehensiveness of our evaluation method. The other results demonstrate that Preemptive Reversion in the white-box setting is the only reversion attack that improves clean accuracy after reversion. The lower numbers in the fourth row suggest that the accuracy decrease observed with Preemptive Reversion in the white-box setting resulted from successful reversion, while other accuracy declines were due to distortion. Consequently, a decrease in accuracy, when solely considered from the fourth row, does not necessarily indicate the success of a reversion attack.

7. Ablation Studies

We conducted an ablation study on the Fast Preemption framework and its learning algorithm using the CIFAR-10 dataset and AutoAttack (Standard) [11] (L_∞ -norm $\epsilon = 8/255$) against a black-box target model, RaWideResNet-70-16 [32]. As shown in Fig. 6, Fast Preemption signif-

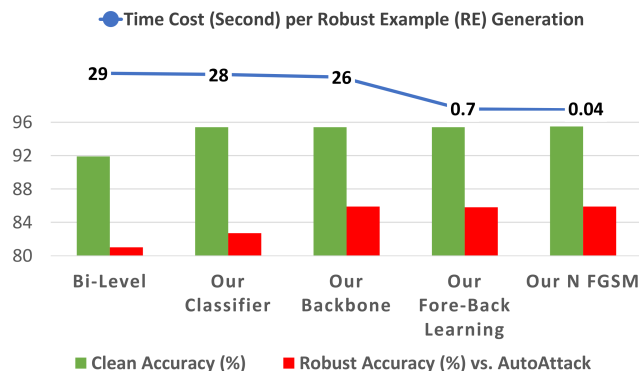


Figure 6. Compared with the SOTA preemptive defense Bi-Level [29], our framework improved the clean and robust accuracies, and our learning algorithm reduced the time cost for defense.

icantly outperforms the SOTA Bi-Level method [29], increasing clean accuracy from 92% to 95.3%, improving robust accuracy from 80.1% to 85.6%, and reducing computation time from 28 seconds to 0.04 seconds. These studies were conducted to identify optimal configurations, with further ablation results provided in Appendix E.

8. Conclusion

We propose Fast Preemption, an efficient, transferable, plug-and-play preemptive adversarial defense that introduces a new layer in the defense hierarchy: Preemptive Defense (ours) \rightarrow Training-Time Defense \rightarrow Test-Time Defense. Fast Preemption minimizes the need for prior knowledge, allowing users to independently safeguard media without relying on third-party interventions. It achieves SOTA clean and robust accuracy among training-time, test-time, and preemptive defenses while addressing the efficiency limitations of existing preemptive approaches, achieving processing speeds up to 700 times faster.

Additionally, we propose Preemptive Reversion, a more robust reversion attack that demonstrates our preemptive defense’s resilience against reversion by incorporating a strategy that maintains the confidentiality of user configurations.

However, our defense exhibits limitations against the proposed reversion attack. While allowing users

to customize defense configurations mitigates reversion attacks, further work aims to simplify user requirements. Future research should also investigate the relationship between backbone models and transferability.

References

- [1] Sravanti Addepalli, Samyak Jain, et al. Efficient and effective augmentation strategy for adversarial training. *Advances in Neural Information Processing Systems (NIPS)*, 35:1488–1501, 2022. 3
- [2] Ian Goodfellow Alex K, Ben Hamner. Nips 2017: Defense against adversarial attack, 2017. 6
- [3] Motasem Alfarra, Juan C Pérez, Ali Thabet, Adel Bibi, Philip HS Torr, and Bernard Ghanem. Combating adversaries with anti-adversaries. In *Proceedings of the AAAI Conference on Artificial Intelligence (AAAI)*, pages 5992–6000, 2022. 2
- [4] Maksym Andriushchenko, Francesco Croce, Nicolas Flammarion, and Matthias Hein. Square attack: a query-efficient black-box adversarial attack via random search. In *European Conference on Computer Vision (ECCV)*, pages 484–501, 2020. 6
- [5] Anish Athalye, Nicholas Carlini, and David Wagner. Obfuscated gradients give a false sense of security: Circumventing defenses to adversarial examples. In *International Conference on Machine Learning (ICML)*, pages 274–283, 2018. 6
- [6] Brian R Bartoldson, James Diffenderfer, Konstantinos Parasyris, and Bhavya Kailkhura. Adversarial robustness limits via scaling-law and human-alignment studies. In *Forty-first International Conference on Machine Learning (ICML) Workshops*, 2024. 1, 2, 6, 7, 3, 4, 5
- [7] Nicholas Carlini and David Wagner. Adversarial examples are not easily detected: Bypassing ten detection methods. In *Proceedings of the 10th ACM Workshop on Artificial Intelligence and Security (AISec)*, pages 3–14, 2017. 1, 3, 6, 2
- [8] Tianlong Chen, Sijia Liu, Shiyu Chang, Yu Cheng, Lisa Amini, and Zhangyang Wang. Adversarial robustness: From self-supervised pre-training to fine-tuning. In *Proceedings of the IEEE/CVF Conference on Computer Vision and Pattern Recognition (CVPR)*, pages 699–708, 2020. 3
- [9] Gilad Cohen, Guillermo Sapiro, and Raja Giryes. Detecting adversarial samples using influence functions and nearest neighbors. In *Proceedings of the IEEE/CVF Conference on Computer Vision and Pattern Recognition (CVPR)*, pages 14453–14462, 2020. 2
- [10] Francesco Croce and Matthias Hein. Minimally distorted adversarial examples with a fast adaptive boundary attack. In *International Conference on Machine Learning (ICML)*, pages 2196–2205, 2020. 6
- [11] Francesco Croce and Matthias Hein. Reliable evaluation of adversarial robustness with an ensemble of diverse parameter-free attacks. In *International Conference on Machine Learning (ICML)*, pages 2206–2216. PMLR, 2020. 2, 6, 7, 8, 3
- [12] Francesco Croce, Maksym Andriushchenko, Vikash Sehswag, Edoardo Debenedetti, Nicolas Flammarion, Mung Chiang, Prateek Mittal, and Matthias Hein. Robustbench: a standardized adversarial robustness benchmark. In *Thirty-fifth Conference on Neural Information Processing Systems Datasets and Benchmarks Track (NeurIPS)*, 2021. 1
- [13] Edoardo Debenedetti, Vikash Sehswag, and Prateek Mittal. A light recipe to train robust vision transformers. In *2023 IEEE Conference on Secure and Trustworthy Machine Learning (SaTML)*, pages 225–253, 2023. 2, 3, 4, 5
- [14] Junhao Dong, Seyed-Mohsen Moosavi-Dezfooli, Jianhuang Lai, and Xiaohua Xie. The enemy of my enemy is my friend: Exploring inverse adversaries for improving adversarial training. In *Proceedings of the IEEE/CVF Conference on Computer Vision and Pattern Recognition (CVPR)*, pages 24678–24687, 2023. 2
- [15] Kevin Eykholt, Ivan Evtimov, Earlene Fernandes, Bo Li, Amir Rahmati, Chaowei Xiao, Atul Prakash, Tadayoshi Kohno, and Dawn Song. Robust physical-world attacks on deep learning visual classification. In *Proceedings of the IEEE conference on computer vision and pattern recognition (CVPR)*, pages 1625–1634, 2018. 1
- [16] Matt Fredrikson, Somesh Jha, and Thomas Ristenpart. Model inversion attacks that exploit confidence information and basic countermeasures. In *Proceedings of the 22nd ACM SIGSAC conference on computer and communications security (ACM CCS)*, pages 1322–1333, 2015. 2
- [17] Iuri Frosio and Jan Kautz. The best defense is a good offense: Adversarial augmentation against adversarial attacks. In *Proceedings of the IEEE/CVF Conference on Computer Vision and Pattern Recognition (CVPR)*, pages 4067–4076, 2023. 1, 3, 6, 7, 2
- [18] Ian J Goodfellow, Jonathon Shlens, and Christian Szegedy. Explaining and harnessing adversarial examples. *arXiv preprint arXiv:1412.6572*, 2014. 1, 2, 5
- [19] Sven Gowal, Sylvestre-Alvise Rebuffi, Olivia Wiles, Florian Stimberg, Dan Andrei Calian, and Timothy A Mann. Improving robustness using generated data. In *Advances in Neural Information Processing Systems (NeurIPS)*, pages 4218–4233, 2021. 2, 6, 1, 3, 4, 5
- [20] Chuan Guo, Mayank Rana, Moustapha Cisse, and Laurens van der Maaten. Countering adversarial images using input transformations. In *International Conference on Learning Representations (ICLR)*, 2018. 2
- [21] Dan Hendrycks, Norman Mu, Ekin Dogus Cubuk, Barret Zoph, Justin Gilmer, and Balaji Lakshminarayanan. Augmix: A simple data processing method to improve robustness and uncertainty. In *International Conference on Learning Representations (ICLR)*, 2019. 6, 1, 2, 5
- [22] Thomas Hickling, Nabil Aouf, and Philippa Spencer. Robust adversarial attacks detection based on explainable deep reinforcement learning for uav guidance and planning. *IEEE Transactions on Intelligent Vehicles*, 2023. 1, 2
- [23] Alex Krizhevsky, Geoffrey Hinton, et al. Learning multiple layers of features from tiny images. Technical report, University of Toronto, 2009. 2, 6, 1
- [24] Bin Liang, Hongcheng Li, Miaoqiang Su, Xirong Li, Wenchang Shi, and Xiaofeng Wang. Detecting adversarial image

- examples in deep neural networks with adaptive noise reduction. *IEEE Transactions on Dependable and Secure Computing*, 18(1):72–85, 2021. 2
- [25] Qinliang Lin, Cheng Luo, Zenghao Niu, Xilin He, Weicheng Xie, Yuanbo Hou, Linlin Shen, and Siyang Song. Boosting adversarial transferability across model genus by deformation-constrained warping. In *Proceedings of the AAAI Conference on Artificial Intelligence (AAAI)*, pages 3459–3467, 2024. 6, 2
- [26] Chang Liu, Yinpeng Dong, Wenzhao Xiang, Xiao Yang, Hang Su, Jun Zhu, Yuefeng Chen, Yuan He, Hui Xue, and Shibao Zheng. A comprehensive study on robustness of image classification models: Benchmarking and rethinking. *International Journal of Computer Vision*, pages 1–23, 2024. 1, 2, 6, 7
- [27] DC Livingston. Colorimetric analysis of the ntsc color television system. *Proceedings of the IRE*, 42(1):138–150, 1954. 7
- [28] Aleksander Madry, Aleksandar Makelov, Ludwig Schmidt, Dimitris Tsipras, and Adrian Vladu. Towards deep learning models resistant to adversarial attacks. In *International Conference on Learning Representations (ICLR)*, 2018. 4, 5, 2, 3
- [29] Seungyong Moon, Gaon An, and Hyun Oh Song. Preemptive image robustification for protecting users against man-in-the-middle adversarial attacks. In *Proceedings of the AAAI Conference on Artificial Intelligence (AAAI)*, pages 7823–7830, 2022. 1, 2, 3, 4, 5, 6, 7, 8
- [30] Maria-Irina Nicolae, Mathieu Sinn, Minh Ngoc Tran, Beat Buesser, Amrisha Rawat, Martin Wistuba, Valentina Zantedeschi, Nathalie Baracaldo, Bryant Chen, Heiko Ludwig, Ian Molloy, and Ben Edwards. Adversarial robustness toolbox v1.2.0. *CoRR*, 2018. 1
- [31] Weili Nie, Brandon Guo, Yujia Huang, Chaowei Xiao, Arash Vahdat, and Animashree Anandkumar. Diffusion models for adversarial purification. In *International Conference on Machine Learning (ICML)*, pages 16805–16827. PMLR, 2022. 1, 2, 3, 6, 7
- [32] ShengYun Peng, Weilin Xu, Cory Cornelius, Matthew Hull, Kevin Li, Rahul Duggal, Mansi Phute, Jason Martin, and Duen Horng Chau. Robust principles: Architectural design principles for adversarially robust cnns. In *British Machine Vision Conference (BMVC)*, 2023. 2, 8, 3, 4, 5, 6
- [33] Rahul Rade and Seyed-Mohsen Moosavi-Dezfooli. Helper-based adversarial training: Reducing excessive margin to achieve a better accuracy vs. robustness trade-off. In *International Conference on Machine Learning (ICML) Workshop on Adversarial Machine Learning (AML)*, 2021. 3
- [34] Edward Raff, Jared Sylvester, Steven Forsyth, and Mark McLean. Barrage of random transforms for adversarially robust defense. In *Proceedings of the IEEE/CVF Conference on Computer Vision and Pattern Recognition (CVPR)*, pages 6528–6537, 2019. 2
- [35] Min Ren, Yuhao Zhu, Yunlong Wang, and Zhenan Sun. Perturbation inactivation based adversarial defense for face recognition. *IEEE Transactions on Information Forensics and Security*, 17:2947–2962, 2022. 3
- [36] Aniruddha Saha, Akshayvarun Subramanya, and Hamed Pirsiavash. Hidden trigger backdoor attacks. In *Proceedings of the AAAI conference on artificial intelligence (AAAI)*, pages 11957–11965, 2020. 1, 2, 4
- [37] Hadi Salman, Andrew Ilyas, Logan Engstrom, Sai Vemprala, Aleksander Madry, and Ashish Kapoor. Unadversarial examples: Designing objects for robust vision. In *Advances in Neural Information Processing Systems (NeurIPS)*, pages 15270–15284, 2021. 3
- [38] Vikash Schwag, Saeed Mahloujifar, Tinashe Handina, Sihui Dai, Chong Xiang, Mung Chiang, and Prateek Mittal. Robust learning meets generative models: Can proxy distributions improve adversarial robustness? In *International Conference on Learning Representations (ICLR)*, 2022. 2, 3
- [39] Ali Shafahi, Mahyar Najibi, Amin Ghiasi, Zheng Xu, John Dickerson, Christoph Studer, Larry S Davis, Gavin Taylor, and Tom Goldstein. Adversarial training for free! In *Proceedings of the 33rd International Conference on Neural Information Processing Systems (NeurIPS)*, pages 3358–3369, 2019.
- [40] Naman D Singh, Francesco Croce, and Matthias Hein. Revisiting adversarial training for imagenet: architectures, training and generalization across threat models. In *Proceedings of the 37th International Conference on Neural Information Processing Systems (NeurIPS)*, pages 13931–13955, 2023. 2, 6
- [41] Rui Tian, Zuxuan Wu, Qi Dai, Han Hu, and Yu-Gang Jiang. Deeper insights into the robustness of vits towards common corruptions. *arXiv preprint arXiv:2204.12143*, 2022. 6, 2
- [42] Deepak Vijaykeerthy, Anshuman Suri, Sameep Mehta, and Ponnurangam Kumaraguru. Hardening deep neural networks via adversarial model cascades. In *2019 International Joint Conference on Neural Networks (IJCNN)*, pages 1–8. IEEE, 2019. 2
- [43] Hanrui Wang, Ruoxi Sun, Cunjian Chen, Minhui Xue, Lay-Ki Soon, Shuo Wang, and Zhe Jin. Iterative window mean filter: Thwarting diffusion-based adversarial purification. *IEEE Transactions on Dependable and Secure Computing*, 2024. 1, 3
- [44] Hanrui Wang, Shuo Wang, Cunjian Chen, Massimo Tistarelli, and Zhe Jin. A multi-task adversarial attack against face authentication. *ACM Transactions on Multimedia Computing, Communications, and Applications*, 20(11), 2024. 1, 2
- [45] Qinglong Wang, Wenbo Guo, Kaixuan Zhang, Alexander G Ororbia, Xinyu Xing, Xue Liu, and C Lee Giles. Adversary resistant deep neural networks with an application to malware detection. In *Proceedings of the 23rd ACM Sigkdd International Conference on Knowledge Discovery and Data Mining (ACM SIGKDD)*, pages 1145–1153, 2017. 2
- [46] Zhou Wang, Alan C Bovik, Hamid R Sheikh, and Eero P Simoncelli. Image quality assessment: from error visibility to structural similarity. *IEEE Transactions on Image Processing*, 13(4):600–612, 2004. 6, 2
- [47] Zekai Wang, Tianyu Pang, Chao Du, Min Lin, Weiwei Liu, and Shuicheng Yan. Better diffusion models further improve adversarial training. In *International Conference on Machine Learning (ICML)*, pages 36246–36263. PMLR, 2023. 2, 3

- [48] Eric Wong, Leslie Rice, and J Zico Kolter. Fast is better than free: Revisiting adversarial training. In *International Conference on Learning Representations (ICLR)*, 2023. [3](#)
- [49] Yuancheng Xu, Yanchao Sun, Micah Goldblum, Tom Goldstein, and Furong Huang. Exploring and exploiting decision boundary dynamics for adversarial robustness. In *International Conference on Learning Representations (ICLR)*, 2023. [3](#)
- [50] Fei Yin, Yong Zhang, Baoyuan Wu, Yan Feng, Jingyi Zhang, Yanbo Fan, and Yujiu Yang. Generalizable black-box adversarial attack with meta learning. *IEEE Transactions on Pattern Analysis and Machine Intelligence*, 2023. [6](#), [2](#)
- [51] Hongyang Zhang, Yaodong Yu, Jiantao Jiao, Eric Xing, Laurent El Ghaoui, and Michael Jordan. Theoretically principled trade-off between robustness and accuracy. In *International Conference on Machine Learning (ICML)*, pages 7472–7482. PMLR, 2019. [1](#), [2](#)
- [52] Richard Zhang, Phillip Isola, Alexei A Efros, Eli Shechtman, and Oliver Wang. The unreasonable effectiveness of deep features as a perceptual metric. In *Proceedings of the IEEE Conference on Computer Vision and Pattern Recognition (CVPR)*, pages 586–595, 2018. [6](#), [2](#)
- [53] Fei Zuo and Qiang Zeng. Exploiting the sensitivity of l2 adversarial examples to erase-and-restore. In *Proceedings of the 2021 ACM Asia Conference on Computer and Communications Security (ACM Asia CCS)*, page 40–51, 2021. [2](#)

Fast Preemption: Forward-Backward Cascade Learning for Efficient and Transferable Preemptive Adversarial Defense

Supplementary Material

This supplementary material provides a detailed exposition of the algorithms underlying the proposed adversarial defense and adaptive reversion attack (Appendix A), outlines the experimental configurations for both attack and defense scenarios (Appendix B), presents evaluation results against a broader range of models (Appendix C), and offers a comprehensive analysis of visual quality (Appendix D). Additionally, it includes an extensive ablation study (Appendix E), examining key components such as the classifier, backbone models, the Forward-Backward Cascade Learning algorithm, and the effectiveness of averaging multiple Fast Gradient Sign Method (FGSM) examples.

A. Detailed Algorithms

The complete defense algorithm of Fast Preemption is presented in Algorithm 1. With PyTorch implementation, Steps 4 to 8 and Steps 15 to 19 can be respectively processed in parallel. The complete adaptive attack algorithm of Preemptive Reversion is presented in Algorithm 2.

B. Experiment Settings

The full experimental settings used for evaluations are listed in Tab. 4. We evaluated attacks and defenses using models with various architectures, as listed in Tab. 5. Our implementation partially leveraged the ART [30] and RobustBench [12] leaderboards by using PyTorch. The experimental machine was equipped with an NVIDIA A100 40GB GPU.

C. Evaluation across More Models

In the main paper, we concentrated on comparisons with top-performing adversarial training methods [6, 26]. In this section, we extend our evaluation to include defenses tested across nine additional victim models on CIFAR-10 [23] from RobustBench [12] in a transferable context. These models encompass diverse architectures representative of platforms such as Twitter and Facebook, differing from both the classifier [21] and the backbone model [19].

As shown in Tab. 6, our method demonstrates significant performance gains compared to no preemptive defense and the SOTA preemptive defense [29]. Specifically, we achieve average improvements of 4.2% and 4.3% in clean accuracy, 17.8% and 5% in robust accuracy, and a 700-fold increase in speed, respectively. Furthermore, compared using the SOTA adversarial training model [6] as the back-

Algorithm 1 Fast Preemption

Input: Original image x , classifier f_c , backbone model f_b , maximum L_∞ -norm distance ϵ , learning rate η , maximum forward steps T_\rightarrow and backward steps T_\leftarrow , number of examples for averaging perturbations N .

Output: Robust example x^r .

```
1: // Forward Propagation
2:  $x_0 = x$ 
3: for  $t < T_\rightarrow$  do
4:   for  $n = 1, \dots, N$  do
5:      $\delta_n \sim U(-\epsilon, +\epsilon)$   $\triangleright$  random initialization
6:      $x_{t,n} = x_t + \delta_n$ 
7:      $x_{t,n}^r = \prod_{x,\epsilon}(x_{t,n} - \epsilon \cdot \text{sign}(\nabla \ell(x_{t,n}|x, f_c, f_b)))$ 
8:      $\triangleright$  FGSM decreases  $\ell$ 
9:   end for
10:   $\delta_t^r = \frac{1}{N} \sum_{n=1}^N x_{t,n}^r - x_t$   $\triangleright$  averages perturbations
11:   $x_{t+1} = x_t + \eta \cdot \delta_t^r$   $\triangleright$  direct enhancement
12: end for
13: // Backward Propagation
14:  $x_0 = x_{T_\rightarrow}$ 
15: for  $t < T_\leftarrow$  do
16:   for  $n = 1, \dots, N$  do
17:      $\delta_n \sim U(-\epsilon, +\epsilon)$   $\triangleright$  random initialization
18:      $x_{t,n} = x_t + \delta_n$ 
19:      $x_{t,n}^a = \prod_{x,\epsilon}(x_{t,n} + \epsilon \cdot \text{sign}(\nabla \ell(x_{t,n}|x, f_c, f_b)))$ 
20:      $\triangleright$  FGSM increases  $\ell$ 
21:   end for
22:   $\delta_t^a = \frac{1}{N} \sum_{n=1}^N x_{t,n}^a - x_t$   $\triangleright$  averages perturbations
23:   $x_{t+1} = x_t - \eta \cdot \delta_t^a$   $\triangleright$  reverses the attack
24: end for
25: return  $x^r = x_{T_\leftarrow}$ 
```

Algorithm 2 Preemptive Reversion

Input: Robust example x^r .

Output: Reversed example \tilde{x} .

```
1:  $(x^r)^r = \text{PreemptiveDefense}(x^r)$   $\triangleright$  secondary defense
2:  $\tilde{x} = x^r - ((x^r)^r - x^r)$   $\triangleright$  reverses the secondary defense
3: return  $\tilde{x}$ 
```

bone model, our chosen [19] yields an average increase of 0.7% in clean accuracy, 2.5% in robust accuracy, and a ten-fold improvement in processing speed.

Table 4. Experiment Settings.

Type	Approach	Settings
Adversarial Attack	PGD [28]	$L_\infty \epsilon = \frac{8}{255}^1 / \frac{4}{255}^2$ or $L_2 \epsilon = 0.5^1 / 2^2$
	AutoAttack [11]	
	CW [7]	
	DeCoW [25]	
	MCG [50]	Maximum Queries = 20,000
Reversion Attack	JPEG	Quality Factor = 50%
	DiffPure [31]	Diffusion Timestep = $0.1^1 / 0.15^2$
	Fast Preemption (ours)	Same with our defense
Defense	DiffPure [31]	Diffusion Timestep = $0.1^1 / 0.15^2$
	Bi-Level [29]	$L_\infty \epsilon = \frac{8}{255}^1 / \frac{4}{255}^2, \eta^3 = 0.1, T_{\leftarrow} = 100, N = 1$
	A^5 [17]	$L_\infty \epsilon = \frac{8}{255}^1 / \frac{4}{255}^2$
	Fast Preemption (ours)	$L_\infty \epsilon = \frac{8}{255}^1 / \frac{4}{255}^2, \eta^3 = 0.7, T_{\rightarrow} = 1, T_{\leftarrow} = 2, N = 20$

¹ for CIFAR-10; ² for ImageNet.

³ η must meet $\eta \cdot (T_{\rightarrow} + T_{\leftarrow}) > 1$.

Table 5. Model architectures.

Dataset	Architecture
CIFAR-10	WideResNet-94-16 [6]
	RaWideResNet-70-16 [32]
	WideResNet-34-20 [29]
	XCiT-L12 [13]
	PreActResNet-18 [19] (backbone) ResNeXt29-32x4d [21] (classifier)
ImageNet	Swin-L [26]
	ConvNeXt-L+ConvStem [40] (backbone) DeiT Base [41] (classifier)

D. Visual Quality

The noise budgets utilized (as detailed in Tab. 4) adhere to standard practices in adversarial machine learning, ensuring the preservation of visual quality and minimizing the likelihood of detection. As illustrated in Fig. 7, for 2,000 images from CIFAR-10 and ImageNet, Structural Similarity Index Measure (SSIM) [46] and Learned Perceptual Image Patch Similarity (LPIPS) [52] scores confirm that the visual quality of our robust examples (REs) is sufficiently high to serve as effective substitutes for the original images. Furthermore, our REs exhibit comparable (often superior) visual quality relative to adversarial examples (AEs) and outputs of existing defense methods.

D.1. Structural Similarity Index (SSIM)

The SSIM is a metric for measuring similarity between two images. It considers luminance, contrast, and structural information. The SSIM between two images x (reference)

and y (distorted) is defined as:

$$SSIM(x, y) = \frac{(2\mu_x\mu_y + C_1)(2\sigma_{xy} + C_2)}{(\mu_x^2 + \mu_y^2 + C_1)(\sigma_x^2 + \sigma_y^2 + C_2)}, \quad (15)$$

where:

- μ_x and μ_y : Mean intensity values of x and y , respectively.
- σ_x^2 and σ_y^2 : Variance of x and y , respectively.
- σ_{xy} : Covariance between x and y .
- C_1 and C_2 : Small constants added to stabilize the metric in the presence of weak denominators, defined as:

$$C_1 = (K_1L)^2, \quad C_2 = (K_2L)^2, \quad (16)$$

where L is the dynamic range of the pixel values (e.g., 255 for 8-bit images), and K_1 and K_2 are small positive constants (commonly, $K_1 = 0.01$ and $K_2 = 0.03$).

The SSIM value ranges from -1 to 1, where:

- 1: Perfect similarity.
- 0: No similarity.
- Negative values indicate dissimilarity.

SSIM is typically calculated locally using a sliding window across the image, and the overall SSIM is the average of local SSIM values. Higher SSIM values denote subtler deviations from the reference images.

D.2. Learned Perceptual Image Patch Similarity (LPIPS)

The LPIPS is a perceptual similarity measure that evaluates the perceptual distance between two images. It uses deep neural network features to compare the visual content and correlates better with human perception than traditional metrics like SSIM.

The LPIPS distance between two images x (reference)

Table 6. Transferable clean and robust accuracy (%) across various victim models against AutoAttack (Standard) [11] with L_∞ -norm perturbations and $\epsilon = 8/255$. All preemptive defenses were conducted using classifier and backbone models distinct from the victim models, even when the architectures were similar.

Model	Metric	No Preemptive Defense	Bi-Level [29]	Fast Preemption (ours)	
Defense Learning	Backbone Time Cost (s)	N/A N/A	Bi-Level [29] 28	WideResNet-94-16 [6] 0.35	PreActResNet-18 [19] 0.04
RaWideResNet-70-16 [32]	Clean	93.5	92.1	95.5	95.4
	Robust	71.4	81.3	86.8	85.9
WideResNet-70-16 [47]	Clean	93.3	91.5	95.5	95.3
	Robust	71.2	80.9	86.4	86.0
WideResNet-34-10 [33]	Clean	91.5	90.2	95.1	95.1
	Robust	62.1	76.2	78.7	80.8
WideResNet-28-10 [49]	Clean	93.4	91.5	95.4	95.6
	Robust	64.8	77.7	81.3	83.2
PreActResNet-18 [48]	Clean	84.2	87.3	90.1	91.6
	Robust	42.4	54.7	55.4	61.2
ResNest152 [38]	Clean	86.9	87.6	91.2	92.4
	Robust	62.4	73.2	75.8	78.2
ResNet-50 [8]	Clean	86.6	88.5	91.6	93.2
	Robust	52.0	68.1	66.7	72.0
ResNet-18 [1]	Clean	86.6	88.1	91.5	92.7
	Robust	51.4	67.5	67.8	72.8
XCiT-L12 [13]	Clean	92.8	91.2	95.1	95.4
	Robust	57.9	71.3	74.6	76.0
Average	Clean	89.9	89.8	93.4	94.1
	Robust	59.5	72.3	74.8	77.3

Bold indicates the best performance.

and y (distorted) is computed as:

$$LPIPS(x, y) = \sum_l \frac{1}{H_l W_l} \sum_{h=1}^{H_l} \sum_{w=1}^{W_l} w_l \|\hat{\phi}_l(x)_{h,w} - \hat{\phi}_l(y)_{h,w}\|_2^2, \quad (17)$$

where:

- l : Layer index in the deep network.
- $\phi_l(x)$: Feature map of x at layer l in the network.
- $\hat{\phi}_l$: Normalized feature maps for each channel.
- H_l, W_l : Height and width of the feature map at layer l .
- w_l : Learned scalar weights for each layer l (trained to match human judgments).

LPIPS uses a pretrained deep neural network to extract feature maps from intermediate layers. The metric normalizes the feature maps and computes the difference between them, weighted according to the learned weights w_l . The LPIPS value typically ranges from 0 (perfect perceptual similarity) to higher values indicating greater dissimilarity. LPIPS provides a perceptually grounded comparison, making it especially useful for evaluating subtle changes in visual quality.

E. Ablation Studies

We conducted ablation studies on the Fast Preemption framework and learning algorithm using the CIFAR-10

dataset. The attacks were PGD [28] and AutoAttack (Standard) [11] with L_∞ -norm perturbations and $\epsilon = 8/255$. As illustrated in Fig. 6 of Sec. 7, Fast Preemption with the proposed framework and learning algorithm outperformed the SOTA benchmark Bi-Level [29] in terms of clean and robust accuracies and time cost. These studies and results were aimed at identifying the optimal strategies.

E.1. Classifier

In all preemptive defenses, correct labeling guarantees that optimization moves in the correct direction. As demonstrated in Tab. 7, a classifier with higher accuracy leads to better performance. As this classifier is not involved in the Fore-Back learning, the time cost of labeling inputs can be ignored compared with that of Fore-Back learning. Note that the use of ground truths is ideal, but this requires manual labeling, which is impractical for efficient user interaction. Therefore, we used the best pretrained classifier in the Fast Preemption framework, one that differs from the backbone model.

E.2. Backbone Model

The backbone model determines the defense time cost and performance. As illustrated in Fig. 8, different backbone models learn different features. To evaluate the effect of the backbone model, we also evaluated white-box defenses, for which the backbone model is the same as the victim model, *i.e.*, paired modules, as stated in Sec. 1, although we

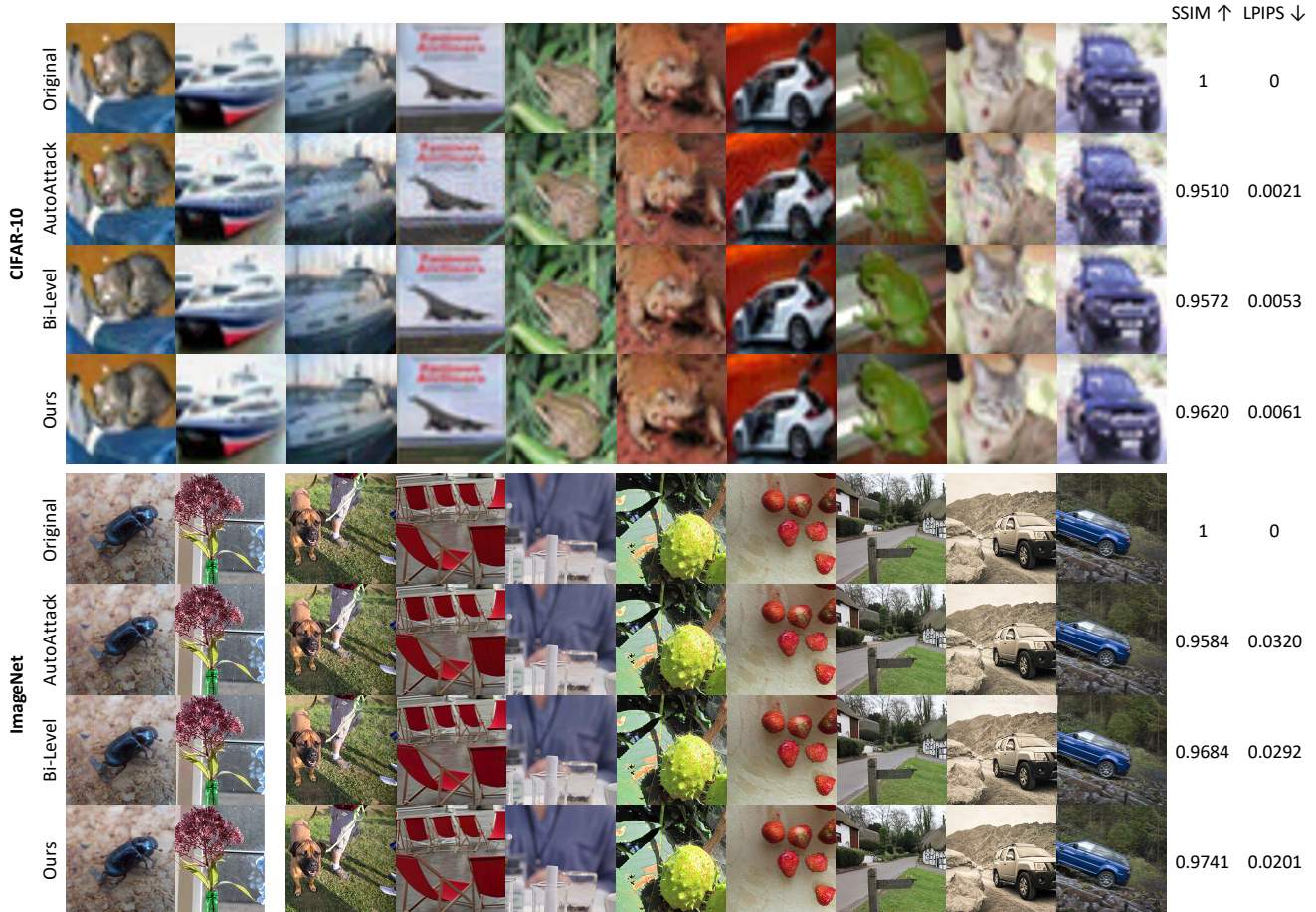


Figure 7. Visual quality of robust examples (REs) generated by our Fast Preemptive defense, compared with adversarial examples (AEs) from AutoAttack and REs from the SOTA preemptive defense [29]. All samples adhere to the same L_∞ -norm constraint ($\epsilon = 8/255$) relative to the original images. SSIM and LPIPS scores demonstrate that the visual quality of our REs is sufficiently high to serve as replacements for the original images, and is comparable to (and often slightly better than) those of the adversarial attack and existing defense methods.

Table 7. Performance with different classifiers.

Classifier	Ablation	Accuracy(%)	Time Cost(s)	Transferable Defense		
				Clean(%)	PGD(%)	AutoAttack(%)
Ground Truths		100	28	97.2	86.9	83.1
ResNeXt		95.9	28	95.4	85.7	82.7
Bi-Level		89.1	29	91.9	83.9	81.0

To evaluate the performance of diverse classifiers in our framework, we used the same backbone model and 100 steps backward propagation as Bi-Level [29]. The transferable defenses were all evaluated using RaWideResNet-70-16 [32] as the victim model. **Bold** indicates the best performance.

believe that this setting is not secure due to potential privacy leakage due to the existence of a backdoor [36].

As shown in Tab. 8, the best adversarially trained model was WideResNet-94-16 [6], so it is not surprising that its white-box defense outperformed that of the other backbone models. However, this most robust model failed to guarantee the best transferability (see results against XCiT-L12 [13]), and the time cost was much higher due to its

complexity. We thus empirically selected PreActResNet-18 [19] as the backbone model in Fast Preemption as it had the least time cost and comparable transferability compared with the SOTA robust model [6]. Nevertheless, it is worth investigating more comprehensive approaches for determining the backbone model in future work.

Table 8. Performance of different backbone models.

	Backbone Model:	Bi-Level [29]	WideResNet-94-16 [6]	PreActResNet-18 [19]
Backbone Robustness	Clean (%)	89.1	93.9	88.1
	PGD (%)	43.9	77.1	61.8
	AutoAttack (%)	42.4	74.0	58.6
Time Cost (s) for Defense		28	69	26
White-Box Defense	Clean (%)	95.5	95.8	93.8
	PGD (%)	84.9	91.6	85.9
	AutoAttack (%)	81.8	90.2	83.3
Transferable Defense Victim: RaWideResNet-70-16 [32]	Clean (%)	95.4	95.5	95.3
	PGD (%)	85.7	89.7	87.6
	AutoAttack (%)	82.7	88.0	85.9
Transferable Defense Victim: XCiT-L12 [13]	Clean (%)	95.3	95.3	95.4
	PGD (%)	72.7	78.6	79.6
	AutoAttack (%)	70.8	75.7	77.3

To evaluate the performance of the backbone models in our framework, we followed the results from the previous section and used ResNeXt29-32x4d [21] as the classifier model, and 100 steps backward propagation as Bi-Level [29]. The transferable defenses were all evaluated using RaWideResNet-70-16 [32] and XCiT-L12 [13] as the victim models, different from the backbone models. **Bold** indicates the best performance.

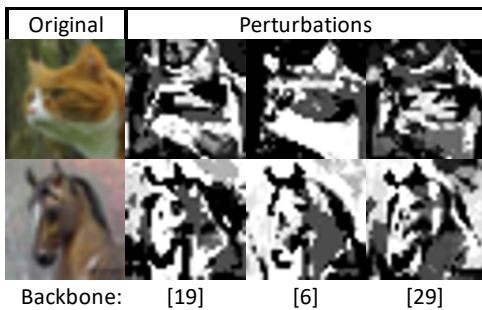


Figure 8. Different backbone models learn different features. PreActResNet-18 [19], WideResNet-94-16 [6], and Bi-Level [29] were adversarially trained, so they learned more crucial features, *i.e.*, ones that are visually similar to the objective.

E.3. Forward-Backward Cascade Learning

As observed in Fig. 9, forward (F) propagation accelerated defense but led to overfitting (*e.g.*, F100-B0). In contrast, backward (B) propagation required more steps to converge (*e.g.*, F0-B100) but alleviated overfitting by the forward propagation (*e.g.*, F10-B90). Additionally, as shown by the curve for “Alternate,” the number of steps in forward propagation must be smaller than that in backward propagation to alleviate overfitting.

Our goal is to reduce the time cost, *i.e.*, learning steps, so we further evaluated forward and backward propagation by limiting the learning steps, as illustrated in Fig. 10. The results show that when the number of learning steps is small, the combination of forward and backward propagation outperforms backward propagation alone (*e.g.*, F1-B2 vs. F0-B3). Therefore, Fast Preemption runs one step forward and two steps backward propagation learning as the

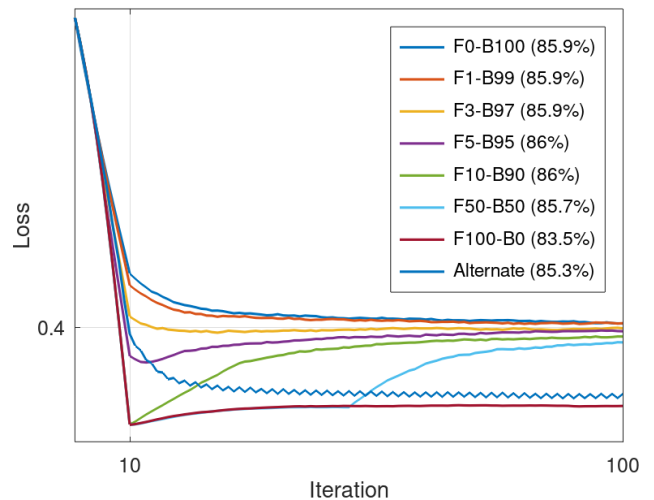


Figure 9. Forward propagation (F) converges faster while backward propagation (B) alleviates overfitting. The numbers following F and B denote the number of learning steps T_{\rightarrow} and T_{\leftarrow} , respectively. The numbers in brackets represent robust accuracy against AutoAttack (Standard). “Alternate” represents the running of forward and backward propagation alternatively for 100 steps in total.

optimal strategy.

E.4. Optimization Algorithm

The results in Tab. 9 indicate that averaging N FGSM examples results in the best performance with the least time cost. Using PGD results in much more time being spent for preemptive defense, whereas using FGSM but without averaging leads to poor performance.

Table 9. Performance for different N and optimization algorithms.

Optimization	Ablation		Time Cost (s)	Clean (%)	Transferable Defense	
	N	Samples			PGD (%)	AutoAttack (%)
PGD	1		0.7	95.3	87.5	85.8
FGSM	1		0.04	95.4	86.8	85.4
PGD	20		0.8	95.2	87.7	85.9
FGSM	20		0.04	95.5	87.8	85.9

Forward propagation ran one step and backward propagation ran two steps. Transferable defense was evaluated using RaWideResNet-70-16 [32] as the victim model. **Bold** indicates the best performance.

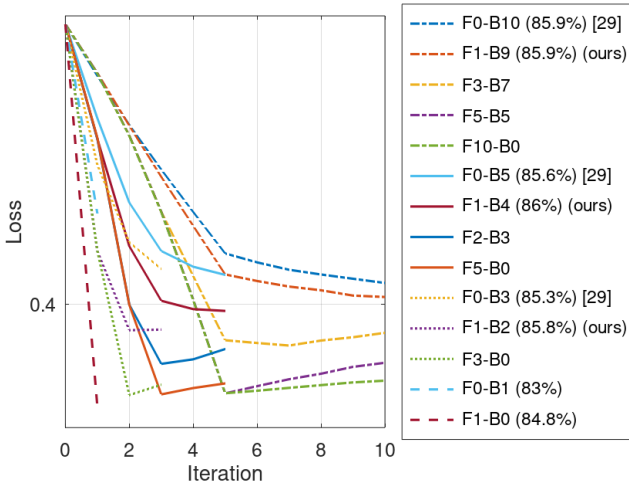


Figure 10. By combining forward (F) and backward (B) propagation, Fast Preemption obtains performance comparable to that of the SOTA preemptive defense [29] by using only three steps (F1–B2). The numbers following F and B denote the number of learning steps T_{\rightarrow} and T_{\leftarrow} , respectively. The numbers in brackets represent robust accuracy against AutoAttack (Standard).